13th World Conference on Earthquake Engineering
Vancouver, B.C., Canada
August 1-6, 2004
Paper No. 2846

A NEW DAMAGE MODEL FOR REINFORCED CONCRETE ELEMENTS

Marlon BAZAN[1] and Mehrdad SASANI[2]

SUMMARY

Utilizing experimental test results on reinforced concrete (RC) elements under cyclic as well as monotonic displacements the Park and Ang damage index is examined. Including the axial force-displacement effects and defining failure as a 20% drop in strength capacity at peak displacement, it is shown that the model is biased against the normalized dissipated energy. A new damage index based on estimating the drift ratio capacity of RC elements under cyclic loading is developed. It is shown that the coefficient of variation in estimating the new damage index at failure is significantly smaller than that reported by Park [1]. It is discussed that although the displacement history can have significant effect on the drift capacity of RC specimens, the dissipated energy may not be a reliable measure to account for such effect.

INTRODUCTION

Designing structures to sustain earthquake demands within the elastic range is usually cost prohibitive. Thus, structures should be provided with sufficient ductility and energy dissipation capacity such that they can undergo inelastic reversal displacements, meeting design requirements. Under severe earthquake ground motions, considerable structural damage without collapse may be allowed. Furthermore, in a multi-level performance-based design or assessment procedure, structures need to satisfy performance requirements under different levels of seismic demand. Therefore, there is a need to quantify damage under different levels of seismic ground motion.

Damage models are main tools to quantify degradation in structures. In general, a damage model is an analytical formulation, in which given the loading history (demand) and mechanical characteristics of a structure (capacity), an index is calculated reflecting damage in the structure. Such an index is called a damage index, *DI*. Damage models may be local, for structural elements, or global, for a whole structure. In this paper only local damage models are studied. Damage indices applications include estimation of losses (human and monetary losses), costs of repair, decision making in post-earthquake assessment (demolition or repair of a damaged structure), disaster planning, insurance costs, evaluation of safety or vulnerability of existing structures and design of new ones.

In general, damage indices (*DI*) vary from 0, indicating no damage, to ≥ 1 indicating failure. For values of *DI* between 0 and 1, some qualitative or quantitative characteristics of expected deterioration need to be

[1]Graduate Research Assistant, [2]Assistant Prof., Northeastern Univ. Boston, USA. Email:sasani@neu.edu

provided. These characteristics could include amount and types of cracks or the crack size, spalling of cover concrete, buckling of reinforcement, crushing of concrete, or reduction in strength capacity. A reliable correlation between *DI* and level of damage will be a valuable tool in multi-level performance-based design. However, in this paper, only the damage index at failure associated with considerable strength degradation is examined.

DEFINITION OF FAILURE

Figure 1 shows the force-displacement relationship for a RC specimen under cyclic displacement. In this paper, it is assumed that failure is reached when, accounting for the axial force-displacement (P-Δ) effects, at least a 20% reduction in the strength is observed. For cyclic tests, a stable cycle is defined as a cycle with drop in strength less than 20% at the peak displacement. The maximum displacement of stable cycles is defined as displacement capacity of the specimen (Figure 1). If the force-displacement relationship of a specimen does not show such a drop in strength, only a lower bound on the displacement capacity is known. Therefore, as far as failure is concerned, such a case is classified as censored data.

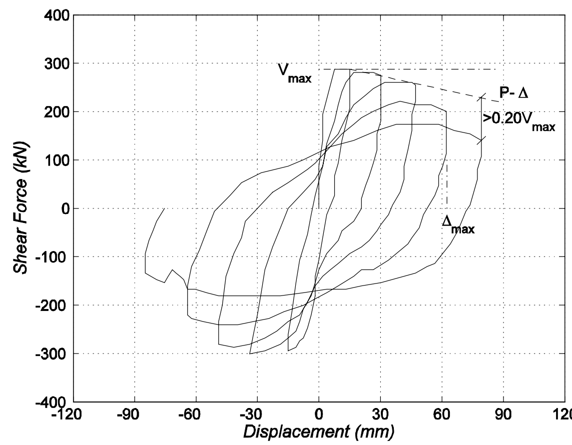

Figure 1. Definition of failure

PARK AND ANG DAMAGE MODEL

The damage model often used for estimating damage index, *DI*, in RC members is developed by Park [1]. The model is defined by a linear combination of normalized maximum displacement and hysteretic energy demands,

$$DI = \frac{\Delta_{max}}{\Delta_u} + \beta \frac{E_h}{F_y \, \Delta_u} \tag{1}$$

where Δ_{max} is the maximum displacement demand under cyclic displacement; Δ_u is the ultimate displacement capacity under monotonic loading; E_h is the hysteretic energy demand under the cyclic displacement; and F_y is the yield strength. For many specimens for which experimental results under cyclic displacements are available, Δ_u is not experimentally known. Therefore, using some available experimental results under monotonic loads and applying a statistical procedure, Park [1] develops a method for estimating Δ_u. The parameter β represents a weighting factor for the effect of energy dissipation on the accumulation of damage. Using experimental test results under cyclic displacement of 261 tests on beams and columns and incorporating the method for estimating Δ_u in a regression analysis, Park [1] suggests an expression for estimating β, which is a function of volumetric transverse reinforcement ratio, shear span to depth ratio, normalized axial force, and tensile reinforcement ratio. Park [1] reported coefficients of variation of 0.60 and 0.54 for estimating β and *DI*, respectively.

Using available experimental test results for RC members tested under cyclic displacements, which have corresponding monotonic tests, the Park and Ang damage model is examined. The main characteristics of the RC specimens are listed in Table 1. Using the exact data, the coefficient of variation of 0.60 is found in estimating *DI* at failure which is comparable with the value reported by Park [1].

Table 1. Experimental set of monotonic and corresponding cyclic tests

Reference	Specimen Monotonic	Specimen Cyclic	f'_c [(1)] (MPa)	ρ_w (%) [(2)]	η_o [(3)]	a/d [(4)]	Mode of Failure [(5)] Monotonic	Mode of Failure [(5)] Cyclic
Watanabe, 1998[2]	302	303	40	0.68	0.00	4.4	S-F	S
Watanabe, 1998[2]	302	304	38	0.68	0.00	4.4	S-F	S
Watanabe, 1998[2]	302	305	38	0.68	0.00	4.4	S-F	S
Watanabe, 1998[2]	302	306	39	0.68	0.00	4.4	S-F	S
Murakami, 1986[3]	C21	C22	24	0.83	0.12	2.8	NA	F
Murakami, 1986[3]	C21	C23	24	0.83	0.12	2.8	NA	F
Murakami, 1986[3]	C21	C24	24	0.83	0.12	2.8	NA	F
Morimoto, 1984[4]	2D16-M	2D16-R	31	1.49	0.16	2.3	F	S
Morimoto, 1984[4]	4D13-M	4D13-R	28	1.49	0.18	2.3	F	S
Mugurama, 1973[5]	E3	F2	34	0.78	0.16	2.3	NA	S-F
Mugurama, 1973[5]	C3	F1	32	0.78	0.18	1.1	NA	S-F
Kokusho, 1972[6]	4A0	4AA0	21	1.31	0.00	1.8	NA	S-F
Kokusho, 1972[6]	4B0	4BB0	21	1.31	0.00	1.8	NA	S-F
Kokusho, 1972[6]	4B0	4BB0-2	21	1.31	0.00	1.8	NA	not failed
Kokusho, 1972[6]	8BX0	8BBX0	21	2.61	0.00	1.8	not failed	S-F
Kokusho, 1972[6]	8B40	8BB40	21	2.61	0.19	1.8	NA	S-F
Wakabayashi, 1971[6]	420M-2	420C	38	0.40	0.00	2.4	S-F	not failed
Wakabayashi, 1971[6]	420M-2	423C	37	0.40	0.43	2.4	not failed	S-F
Wakabayashi, 1971[6]	443M	443C	38	0.80	0.39	2.4	S-F	S-F
Wakabayashi, 1971[6]	445M	445C	38	0.80	0.60	2.4	S-F	S-F
Wakabayashi, 1971[6]	620M	620C-2	37	0.40	0.00	3.6	not failed	S
Wakabayashi, 1971[6]	623M-2	623C	38	0.40	0.40	3.5	S-F	S-F
Wakabayashi, 1971[6]	623M-2	623D	40	0.40	0.37	3.5	S-F	S-F
Wakabayashi, 1971[6]	643M	643C	33	0.79	0.39	3.5	not failed	S-F
Wakabayashi, 1971[6]	643M	643D	34	0.79	0.38	3.5	not failed	S-F
Brown, 1970[7]	66-35-M	66-35-RV5	39	1.60	0.00	6.1	not failed	F
Brown, 1970[7]	66-35-M	66-35-RV10	37	1.60	0.00	6.1	not failed	F
Brown, 1970[7]	88-35-M	88-35-RV5	41	1.60	0.00	6.2	S-F	F
Brown, 1970[7]	88-35-M	88-35-RV10	39	1.60	0.00	6.2	S-F	F
Ikeda, 1968[8]	O6	O3	21	0.72	0.19	2.9	not failed	F
Ikeda, 1968[8]	O6	O4	21	0.72	0.19	2.9	not failed	F
Ikeda, 1968[8]	O8	O5	21	0.78	0.48	2.9	S-F	S
Ikeda, 1968[8]	O8	O7	21	0.78	0.48	2.9	S-F	S
Burns, 1962[9]	J-8	J-3	34	1.23	0.00	6.6	F	F
Burns, 1962[9]	J-6	J-7	31	0.97	0.00	3.7	S-F	S-F
Burns, 1962[9]	J-5	J-12	31	0.97	0.00	3.7	F	F

(1) f_c' : concrete compressive strength (*MPa*)

(2) ρ_w : ratio of volume of transverse reinforcement to concrete core volume

(3) $\eta_o = P/Ag\, f_c'$: where P is applied axial load and Ag is cross sectional area of specimen

(4) a/d : aspect ratio; where a is shear span and d is effective depth of section

(5) Mode of Failure: F=flexural; S=shear; and S-F=shear-flexural

A value of β=0.05 for RC beams and columns is suggested by Park [10] along with an expression for estimating Δ_u. Cosenza [11] have pointed out that the experimental values of β for the specimens used for developing the Park and Ang [1] damage model ranged between -0.3 to +1.2 with a median of 0.15. Figure 2 shows normalized dissipated energy, $E_h/F_y\Delta_u$, versus (1- Δ_{max}/Δ_u). As it can be seen, assuming β=0.05, the model significantly underestimates the experimental results. Assuming β=0.15, the model underestimates the *DI* for small values of normalized dissipated energy (even for specimens that did not failed monotonically, that should be overestimated) and overestimates the *DI* for large values of normalized dissipated energy. Thus, such a model with constant β is biased against normalized dissipated energy. In fact, if (1) is simplified to $DI = \Delta_{max}/\Delta_u + \alpha$, α≈0.5 results in a significant reduction of the coefficient of variation in predicting the *DI* (Sasani [12]).

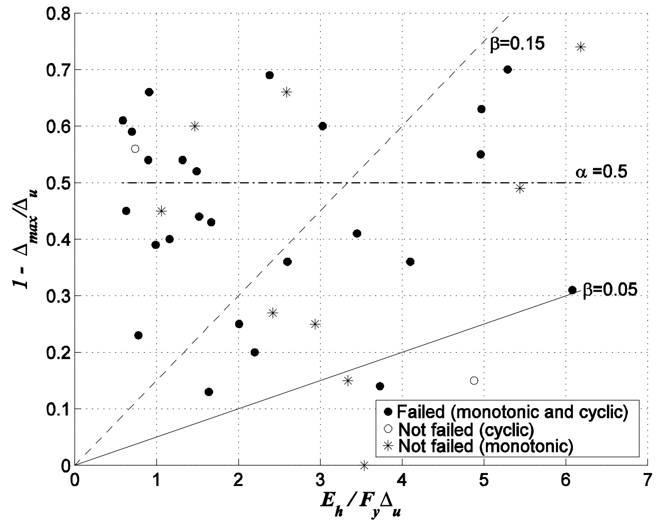

Figure 2. Relationship between normalized dissipated energy and normalized cyclic displacement capacity.

DEFORMATION CAPACITY MODEL

In this section a model is proposed for estimating the drift ratio capacity, DR_c, of RC elements. Drift ratio, *DR*, is defined as the lateral tip displacement divided by the length of the element.

Deformation of RC elements

Deformation of RC elements under lateral loads consists of flexural, bond slip, and shear components. The tip flexural displacement capacity, Δ_f, of a fixed base cantilever of length *a*, can be written as:

$$\Delta_f = \Delta_y + \Delta_p \tag{2}$$

where Δ_y and Δ_p are the yield displacement and plastic displacement, respectively. The plastic displacement can be found from (Paulay [13])

$$\Delta_p = \Phi_p L_p \left(a - L_p/2\right) \tag{3}$$

where Φ_p is the maximum plastic curvature and L_p is the plastic hinge length. Given that the plastic hinge length is small compared to the length of RC elements, $\left(a - L_p/2\right)$ in (3) can be approximated by *a*. Therefore, from (2) and (3) we obtain

$$DR_f = DR_y + \Phi_p L_p \tag{4}$$

where DR_f and DR_y are the total flexural and yield drift ratios, respectively. Another source of deformation is the bond slip in the foundation and the resulting rotation at the base of the cantilever. One can account for the deformation due to the bond slip explicitly or by adjusting the plastic hinge length (Paulay [13]).

The drift ratio due to shear deformation (DR_s) of cracked RC elements can be calculated using the relationship proposed by Park [14]

$$DR_s = \left(\frac{1}{\rho_v} + 4n \right) \frac{V_s}{E_s\, b_w\, d} \tag{5}$$

where ρ_v is the shear reinforcement ratio, n is the ratio of modulus of elasticity of steel and concrete, V_s is the shear transferred through the truss action, E_s is the modulus of elasticity of steel, and b_w and d are the width of the web and the effective depth of the section, respectively.

Experimental results

Experimental results of 159 RC specimens having rectangular sections subjected to cyclic displacements are used to develop a model for estimating deformation capacity of RC elements. The ranges of the main characteristics of the specimens are listed in Table 2. Parameters $f_c^{'}$, ρ_w, η_o, and a/d are defined in Table 1. The longitudinal reinforcement ratio, ρ_t, is defined as the tensile reinforcement divided by *bd*. The shear stress coefficient is defined as $V/(A_g\sqrt{f_c^{'}})$, where V is the maximum shear force applied to the specimen. As it can be seen, the specimens have wide ranges of main characteristics.

Table 2. Ranges of main characteristics of RC specimens

Characteristics	Range
$f_c^{'}$ *(MPa)*	16.0 – 48.3
ρ_w *(%)*	0.16 – 3.78
η_o	0.00 – 0.60
a/d	1.2 – 8.9
ρ_t *(%)*	0.52 – 2.70
$V/(A_g\sqrt{f_c^{'}})$*	0.087 – 0.72
DR_c *(%)*	0.61 – 11.5

*V in MN, A_g in m^2, and $f_c^{'}$ in MPa. A unit value here, corresponds to 12 units if V in lb, A_g in in^2, and $f_c^{'}$ in psi.

A complete list of the specimens is given in Table 3. Figure 3 represents the different types of test setups specified in Table 3. Note that for tests reported in [16], [20] and [44], the test setups are considered as cantilevers. The main characteristics of the specimens are shown in Figure 4. The experimental data was obtained from the database compiled by Eberhard [15] and from other references that are cited in this paper.

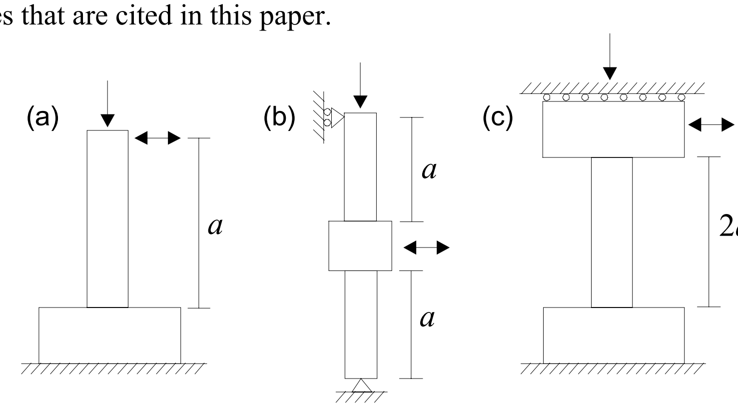

Figure 3. Test setups: cantilever (a); double ended (b); and double curvature (c)

Effects of different parameters on deformation capacity of RC elements

Main parameters affecting (4) are the amount and mechanical characteristics of transverse and longitudinal reinforcement, amount of axial force as well as geometric characteristics of elements. In Figure 5(a), data points connected by solid lines represent experimental results of specimens with similar characteristics but different amounts of volumetric transverse reinforcement, ρ_w, subjected to similar cyclic displacement histories. Note that the mode of failure for each specimen is identified. Similarly, Figure 5(b), (c) and (d) show the drift ratio capacity for specimens that differ only in η_o, *a/d*, and, ρ_t, respectively. Effects of these parameters on deformation capacity of RC elements are examined below.

Table 3. Test specimens

No.	Specimen	Reference	T.S.(1)	Fail. (2)	Type(3)
1	D1N30	Bechtoula, 2002[15]	C	F	E
2	D1N60	Bechtoula, 2002[15]	C	F	E
3	L1N60	Bechtoula, 2002[15]	C	F	E
4	L1N6B	Bechtoula, 2002[15]	C	F	E
5	10-1-2.25N	Pujol, 2002[16]	C	F	E
6	10-1-2.25S	Pujol, 2002[16]	C	F	E
7	10-2-2.25N	Pujol, 2002[16]	C	F	E
8	10-2-2.25S	Pujol, 2002[16]	C	F	E
9	10-2-3N	Pujol, 2002[16]	C	F	E
10	10-2-3S	Pujol, 2002[16]	C	F	E
11	10-3-1.5N	Pujol, 2002[16]	C	F	E
12	10-3-1.5S	Pujol, 2002[16]	C	F	E
13	10-3-2.25N	Pujol, 2002[16]	C	F	E
14	10-3-2.25S	Pujol, 2002[16]	C	F	E
15	10-3-3N	Pujol, 2002[16]	C	F	E
16	10-3-3S	Pujol, 2002[16]	C	F	E
17	20-3-3N	Pujol, 2002[16]	C	F	E
18	20-3-3S	Pujol, 2002[16]	C	F	E
19	1	Sezen, 2002[17]	DC	S-F	E
20	C1-1	Mo, 2000[18]	C	F	E
21	C1-2	Mo, 2000[18]	C	F	E
22	C1-3	Mo, 2000[18]	C	F	E
23	C2-1	Mo, 2000[18]	C	F	E
24	C2-2	Mo, 2000[18]	C	F	E
25	C2-3	Mo, 2000[18]	C	F	E
26	C3-1	Mo, 2000[18]	C	F	E
27	C3-2	Mo, 2000[18]	C	F	E
28	C3-3	Mo, 2000[18]	C	F	E
29	SC3	Aboutaha, 1999[19]	C	S	E
30	SC9	Aboutaha, 1999[19]	C	S	E
31	C5-00N	Matamoros, 1999[20]	C	F	E
32	C5-00S	Matamoros, 1999[20]	C	F	E
33	C5-20N	Matamoros, 1999[20]	C	F	E
34	C5-20S	Matamoros, 1999[20]	C	F	E
35	C5-40N	Matamoros, 1999[20]	C	F	E
36	C5-40S	Matamoros, 1999[20]	C	F	E
37	BG-1	Saatcioglu, 1999[21]	C	F	E
38	BG-2	Saatcioglu, 1999[21]	C	F	E
39	BG-3	Saatcioglu, 1999[21]	C	F	C
40	BG-4	Saatcioglu, 1999[21]	C	F	E
41	BG-5	Saatcioglu, 1999[21]	C	F	E
42	BG-6	Saatcioglu, 1999[21]	C	F	E
43	BG-7	Saatcioglu, 1999[21]	C	F	E
44	BG-8	Saatcioglu, 1999[21]	C	F	E
45	BG-9	Saatcioglu, 1999[21]	C	F	E
46	BG-10	Saatcioglu, 1999[21]	C	F	C
47	A1	Wehbe, 1998[22]	C	F	E
48	A2	Wehbe, 1998[22]	C	F	E
49	B1	Wehbe, 1998[22]	C	F	E
50	B2	Wehbe, 1998[22]	C	F	E
51	2CLH18	Lynn, 1996[23]	DC	S-F	E
52	2CMH18	Lynn, 1996[23]	DC	S-F	E
53	3CLH18	Lynn, 1996[23]	DC	S	E
54	3CMD12	Lynn, 1996[23]	DC	S	E
55	3CMH18	Lynn, 1996[23]	DC	S	E
56	2SLH18	Lynn, 1996[23]	DC	S-F	E
57	3SLH18	Lynn, 1996[23]	DC	S	E
58	3SMD12	Lynn, 1996[23]	DC	S-F	E
59	1	Nosho, 1996[24]	C	F	E
60	9	Park 1990[25]	C	F	C
61	1	Tanaka, 1990[26]	DE	F	C
62	2	Tanaka, 1990[26]	DE	F	C
63	4	Tanaka, 1990[26]	DE	F	C
64	5	Tanaka, 1990[26]	C	F	C
65	6	Tanaka, 1990[26]	C	F	C
66	7	Tanaka, 1990[26]	C	F	C
67	8	Tanaka, 1990[26]	C	F	C
68	OA2	Arakawa, 1989[27]	DC	S	E
69	OA5	Arakawa, 1989[27]	DC	S	E
70	CA025C	Ono, 1989[28]	DC	S-F	E
71	U1	Saatcioglu, 1989[29]	C	F	E
72	U3	Saatcioglu, 1989[29]	C	F	E
73	U4	Saatcioglu, 1989[29]	C	F	E
74	U6	Saatcioglu, 1989[29]	C	F	E
75	U7	Saatcioglu, 1989[29]	C	F	E
76	5	Watson, 1989[30]	DE	F	E
77	6	Watson, 1989[30]	DE	F	E
78	NC-2	Azizinamini, 1988[31]	DE	F	E
79	NC-4	Azizinamini, 1988[31]	DE	F	E
80	85PDC-1	Kanda, 1988[32]	DC	F	C
81	85PDC-2	Kanda, 1988[32]	DC	F	C
82	85PDC-3	Kanda, 1988[32]	DC	F	C
83	85STC-1	Kanda, 1988[32]	DC	F	E

Table 1. Test specimens (Continued)

No.	Specimen	Reference	T.S.(1)	Fail.(2)	Type(3)
84	85STC-2	Kanda, 1988[32]	DC	F	E
85	1	Imai, 1986[33]	DC	S	E
86	C22	Murakami, 1986[3]	C	F	E
87	C23	Murakami, 1986[3]	C	F	E
88	C24	Murakami, 1986[3]	C	F	E
89	1	Soesianawati, 1986[34]	DE	F	E
90	2	Soesianawati, 1986[34]	DE	F	E
91	3	Soesianawati, 1986[34]	DE	F	E
92	4	Soesianawati, 1986[34]	DE	F	E
93	7	Zahn, 1986[35]	DE	F	E
94	8	Zahn, 1987[35]	DE	F	E
95	1	Bett, 1985[36]	DC	S	E
96	2D16RS	Ohue, 1985[37]	DC	S-F	E
97	4D13RS	Ohue, 1985[37]	DC	S-F	E
98	2D16-R	Morimoto, 1984[4]	DC	S	E
99	4D13-R	Morimoto, 1984[4]	DC	S	E
100	L1	Ohno, 1984[38]	C	F	C
101	L2	Ohno, 1984[38]	C	F	C
102	L3	Ohno, 1984[38]	C	F	E
103	HPRC10-63	Nagasaka, 1982[39]	DC	S	E
104	HPRC19-32	Nagasaka, 1982[39]	DC	S-F	E
105	2CUS	Umehara, 1982[40]	DC	S	E
106	CUS	Umehara, 1982[40]	DC	S	E
107	CUW	Umehara, 1982[40]	DC	S	E
108	3	Ghee, 1981[41]	DE	F	C
109	4	Ghee, 1981[41]	DE	F	C
110	1	Gill, 1979[42]	DE	F	C
111	2	Gill, 1979[42]	DE	F	C
112	3	Gill, 1979[42]	DE	F	C
113	4	Gill, 1979[42]	DE	F	C
114	1	Atalay, 1975[43]	DE	F	C
115	2	Atalay, 1975[43]	DE	F	C
116	3	Atalay, 1975[43]	DE	F	C
117	4	Atalay, 1975[43]	DE	F	E
118	5	Atalay, 1975[43]	DE	F	E
119	6	Atalay, 1975[43]	DE	F	E
120	9	Atalay, 1975[43]	DE	F	E
121	10	Atalay, 1975[43]	DE	F	E
122	11	Atalay, 1975[43]	DE	F	E
123	12	Atalay, 1975[43]	DE	F	E
124	F2	Mugurama, 1973[5]	DC	S-F	E
125	25.033E	Wight, 1973[44]	C	S	E
126	25.033W	Wight, 1973[44]	C	S-F	E
127	40.033aE	Wight, 1973[44]	C	S-F	E
128	40.033E	Wight, 1973[44]	C	S-F	E
129	40.033W	Wight, 1973[44]	C	S-F	E
130	40.048E	Wight, 1973[44]	C	S-F	E
131	40.048W	Wight, 1973[44]	C	S-F	E
132	40.067E	Wight, 1973[44]	C	S-F	E
133	40.067W	Wight, 1973[44]	C	S-F	E
134	40.092E	Wight, 1973[44]	C	S-F	E
135	40.092W	Wight, 1973[44]	C	S-F	E
136	40.147E	Wight, 1973[44]	C	S-F	C
137	40.147W	Wight, 1973[44]	C	S-F	C
138	4AA0	Kokusho, 1972[6]	DC	S-F	E
139	4BB0	Kokusho, 1972[6]	DC	S-F	E
140	4BB0-2	Kokusho, 1972[6]	DC	S-F	C
141	8BBX0	Kokusho, 1972[6]	DC	S-F	E
142	8BB40	Kokusho, 1972[6]	DC	S-F	E
143	420C	Wakabayashi, 1971[6]	DC	S-F	C
144	423C	Wakabayashi, 1971[6]	DC	S-F	E
145	443C	Wakabayashi, 1971[6]	DC	S-F	E
146	445C	Wakabayashi, 1971[6]	DC	S-F	E
147	620C-2	Wakabayashi, 1971[6]	DC	S	E
148	623C	Wakabayashi, 1971[6]	DC	S-F	E
149	623D	Wakabayashi, 1971[6]	DC	S-F	E
150	643C	Wakabayashi, 1971[6]	DC	S-F	E
151	643D	Wakabayashi, 1971[6]	DC	S-F	E
152	66-35-	Brown, 1970[7]	C	F	E
153	66-35-RV5	Brown, 1970[7]	C	F	E
154	88-35-	Brown, 1970[7]	C	F	E
155	88-35-RV5	Brown, 1970[7]	C	F	E
156	O3	Ikeda, 1968[8]	DE	F	E
157	O4	Ikeda, 1968[8]	DE	F	E
158	O5	Ikeda, 1968[8]	DE	S	E
159	O7	Ikeda, 1968[8]	DE	S	E

(1) Test setup: C=cantilever; DC=double curvature; and DE=double ended

(2) Mode of failure: F=flexural; S-F=shear-flexural; and S=shear

(3) Type of data: E=exact; and C=censored

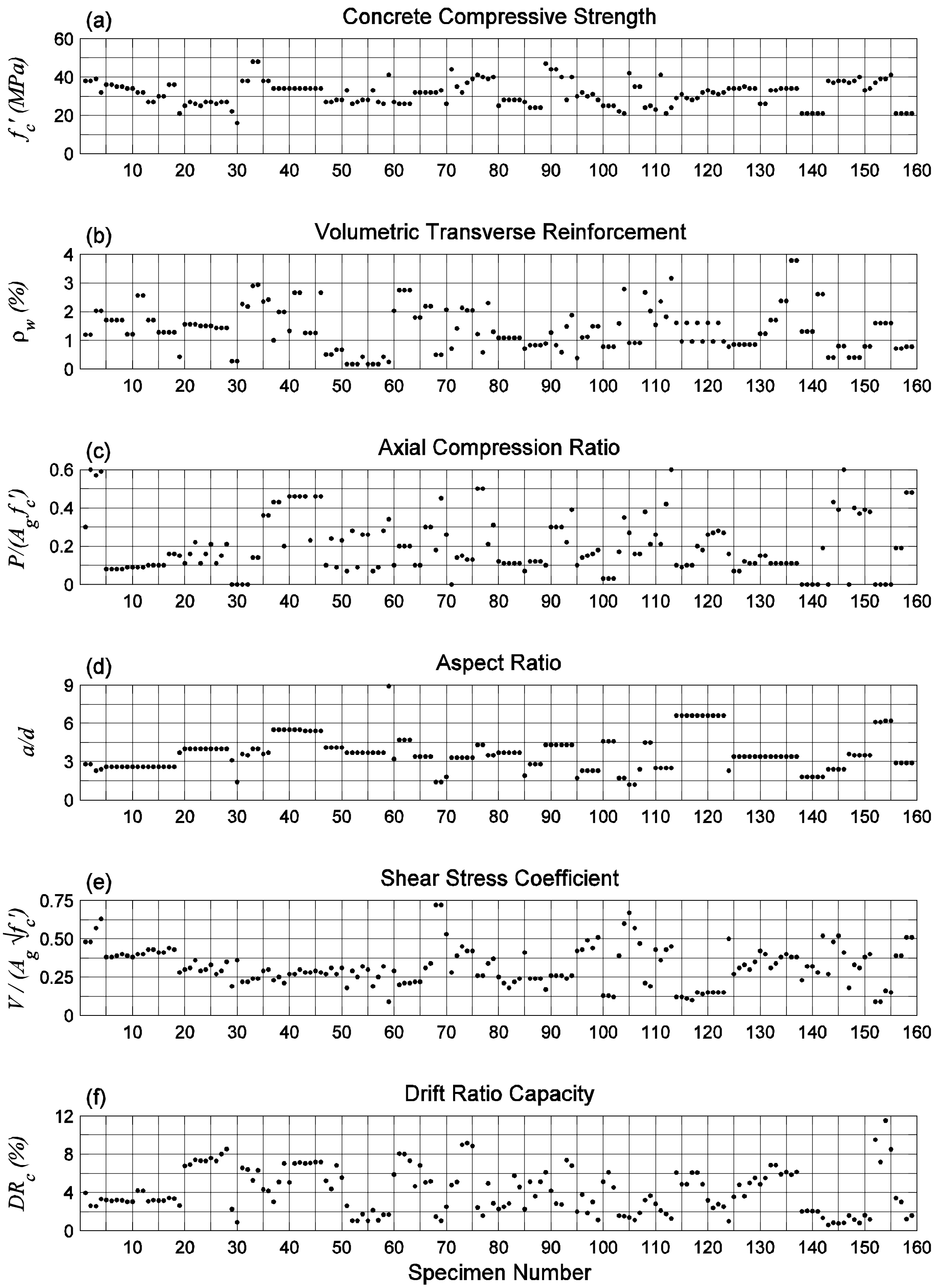

Figure 4. Main characteristics of test specimens

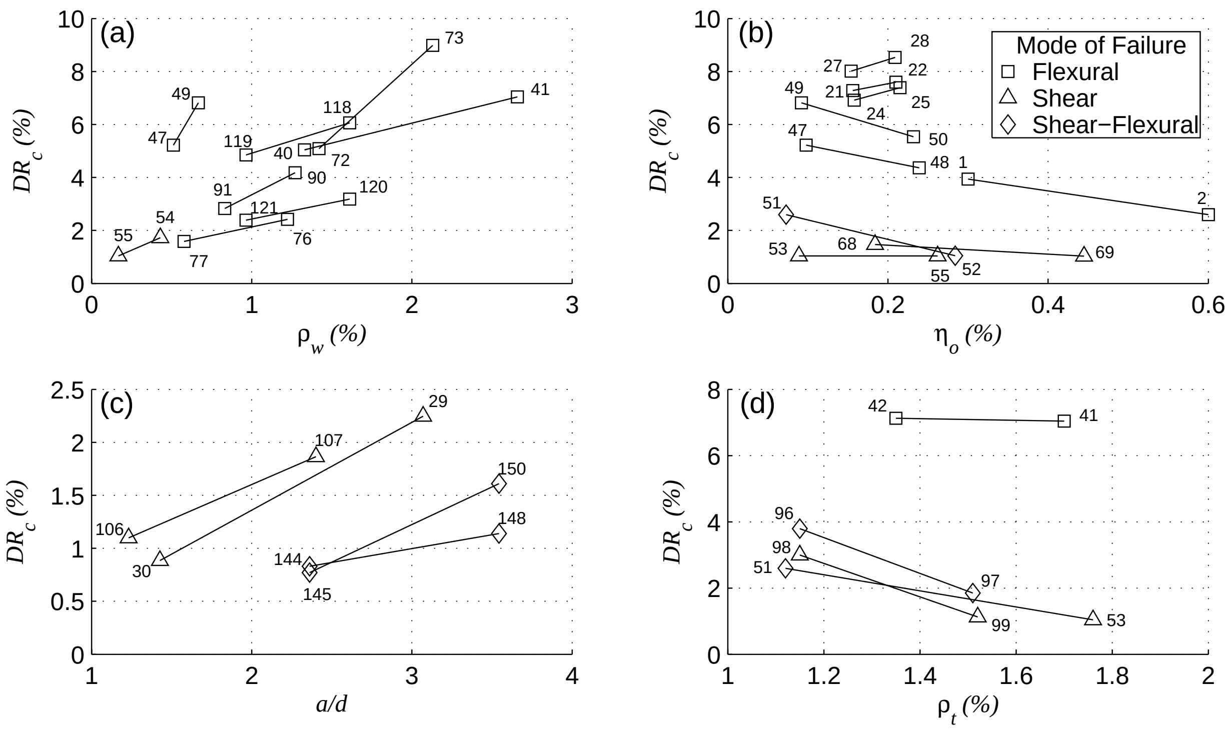

Figure 5. Effects of different parameters on drift capacity

Transverse reinforcement

The amount of transverse reinforcement directly affects the ultimate curvature of RC sections which in turn affects the drift ratio capacity of elements (see Equation 4). Transverse reinforcement also affects the shear deformation (see Equation 5) of RC elements. The effect of ρ_w on drift ratio capacity, DR_c, can be seen in Figure 5(a). As shown, an increase in ρ_w results in larger drift ratio capacity in all cases.

Axial load

The amount of axial load directly affects the depth of the compressive zone and the ultimate curvature of RC sections which in turn affects the drift capacity of elements (see Equation 4). Figure 5(b) shows effect of axial load on drift ratio capacity. As it can be seen, except for specimens 21-22, 24-25 and 27-28, increasing the axial load results in smaller drift ratio capacity.

Aspect Ratio

Figure 5(c) shows the effect of *a/d* on drift ratio capacity. For all the cases, an increase in the drift ratio capacity as a result of an increase in the aspect ratio is observed.

Longitudinal reinforcement

Figure 5(d) shows the effect of longitudinal reinforcement ratio on drift ratio capacity. As it can be seen, except for specimens 41-42, increasing the longitudinal reinforcement results in smaller drift ratio capacity.

Drift ratio capacity model

For a cantilever having uniform section properties, the elastic flexural deformation under a tip lateral load can be calculated using a linear curvature distribution over the length of the element. However, in RC elements because of the formation of cracks, mainly at the vicinity of the base where the bending moment is maximum, there is a significant reduction in the flexural stiffness of sections in that region. As a result, the tip yield deformation is mainly due to curvature in the vicinity of the base. Therefore similar to plastic drift ratio, the yield drift ratio can be estimated from $DR_y = \Phi_y L_y$, where L_y is some portion of length of the element. Given that the ultimate curvature is $\Phi_u = \Phi_y + \Phi_p$, (4) can be rewritten as

$$DR_f = \Phi_u L_p^* \tag{6}$$

where L_p^* is a length that can be considered as a weighted average between L_p and L_y.

Figure 6 shows the ratio of shear to total deformations at failure of specimens tested by Pujol [16] and Atalay [43] that failed in flexure and the specimens tested by Lynn [23][45] that failed in shear. The mean value of shear to total deformation, *m*, for each set is also shown in the Figure 6. As it can be seen, while *m* for tests conducted by Pujol [16] is 15.4%, the value for tests carried out by Atalay [43] is only 3.3%. This is mainly attributed to the fact that the shear span ratio (a/d) in the former case is about 2.6, while in the latter case is 6.6. Larger value of *m=17.7%* is found in tests conducted by Lynn [23][45] in which specimens failed in shear.

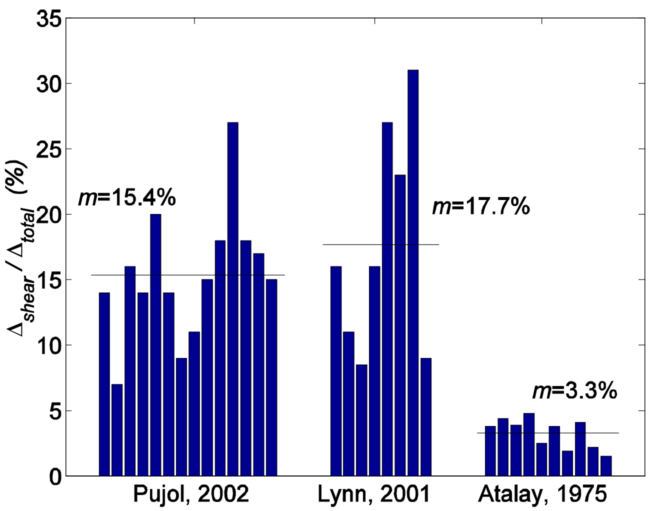

Figure 6. Contribution of shear deformation in total deformation

In order to develop a model that is not too complex yet can reliably estimate the drift capacity of RC elements that failed either in flexure or in shear, and given the fact that the shear deformation is a small portion of the total deformation, let us first examine (6). The ultimate curvature in (6) can be limited by the maximum concrete usable strain, which in turn is significantly affected by ρ_w. In other words, the larger the ρ_w, the larger the Φ_u becomes. Moreover, η_0 directly affects the depth of the compressive zone and therefore affects the ultimate curvature. Therefore, one can assume that $\Phi_u \propto \rho_w^{\alpha}\ \eta_0^{\gamma}$, where α and γ are parameters. Similar to the plastic hinge length, L_p^* can be considered to be proportional to the shear span of elements (Paulay [13]). Moreover, in order to account for the bond slip, one can assume that L_p^* is a linear function of *a*. Given the fact that the test results indicate a direct relationship between *a/d* and the drift ratio capacity and the fact that *a/d* can be used as a measure to identify the relative importance of the flexural and shear response of RC elements, it is decided to replace L_p^* with $\lambda_1 \dfrac{a}{d} + \lambda_2$, where λ_1 and λ_2 are parameters.

$$\hat{DR}_c = \theta\, \rho_w^{\alpha}\ \eta_0^{\gamma} \left(\lambda_1 \frac{a}{d} + \lambda_2 \right) \tag{7}$$

The superposed hat on the drift ratio capacity signifies that the model is not exact and is subjected to error. θ is set equal to one for cantilever elements and need to be estimated for double curvature and double-ended elements. Figure 7 shows the concentration of deformation on one end of double curvature and double ended specimens. In such specimens, if damage is concentrated on one end, the drift capacity will be mainly due to the deformation on the damaged end. Therefore, compared to a similar cantilever specimen, the drift capacity is expected to be smaller. The parameter θ is included in the model to account for such a difference between cantilever specimens and double curvature and double ended specimens.

Note that, because the contribution of shear deformation in total deformation is not significant (see Figure 6), the shear deformation is not explicitly accounted for in the model. However, ρ_w, *a/d,* as well as η_0, which are used in (7), affect shear deformation as discussed in the examination of the experimental data (Figure 5) and in (5).

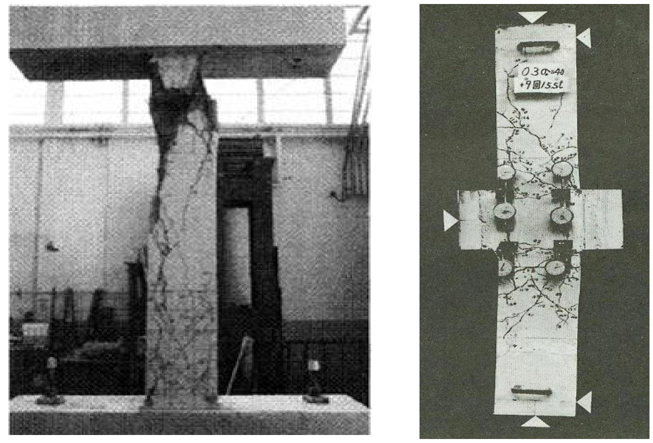

Figure 7. Concentration of deformation in top part of a double curvature specimen (Lynn [23]), left; and in bottom part of a double ended specimen (Ikeda [8])

DAMAGE INDEX

The drift capacity model proposed in this paper is used to develop a new damage model. The model is defined as

$$\hat{DI} = \frac{DR_d}{\hat{DR}_c} \tag{8}$$

where DR_d is the maximum drift ratio demand under cyclic loading and $\hat{DR}_c$ is found from (7). Again the superposed hat on the damage index signifies that the model is not exact and is subjected to error.

Estimation of parameters

In order to estimate the parameters of the model in (7) and (8), the Bayesian parameter estimation technique is used. A brief description of the technique can be found in Sasani [46]. The technique utilizes not only the experimental data that are exact, i.e. the failure is observed, but also uses the specimens in which failure (a 20% drop in strength capacity) did not occur. Accounting for the error in (8) and after proper transformation, the model can be written as

$$DI = e^{\varepsilon}\left(\frac{DR_d}{\hat{DR}_c}\right) \tag{9}$$

where ε is the model error which has normal distribution with zero mean and standard deviation σ. The mean values of the parameters are given in Table 4. In addition to the parameters used in the model, limits are also imposed on ρ_w, η_0, and *a/d*. For ρ_w > 2.0%, use ρ_w = 2.0%. Note that the smallest value of ρ_w used to develop the model is 0.16%. For *a/d* < 2.3 use *a/d* = 2.3 and for *a/d* > 4.5 use *a/d*=4.5. Also for η_0< 0.13 use η_0=0.13. Note that as expected, the value of θ is considerably less than one. Also note that the standard deviation of the error term is only 0.29. Figure 8 shows the error in predicting the *DI* at failure (*DI*=1) for 159 RC specimens. The coefficient

Table 4. Mean value of parameters

Parameter	Mean Value
θ	0.73
α	0.56
γ	-0.43
λ_1	0.92
λ_2	-1.04
σ	0.29

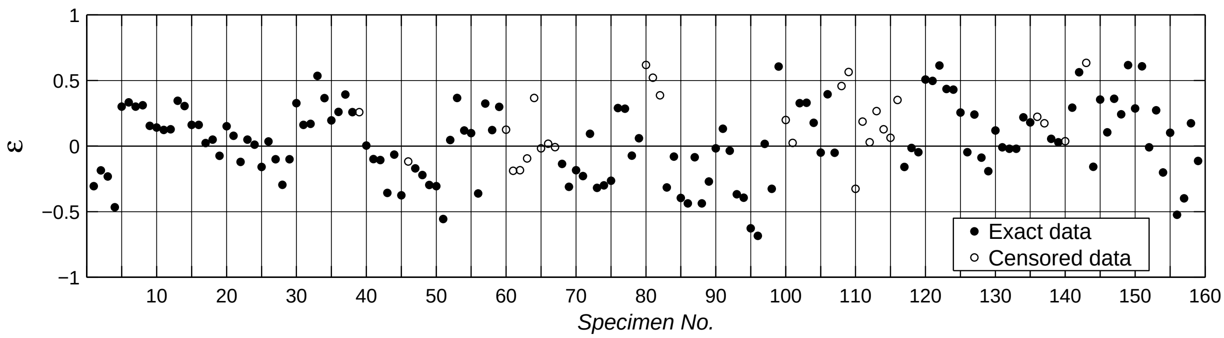

Figure 8. Error in estimating *DI* at failure

of variation in predicting the *DI* at failure is approximately equal to 0.30. This coefficient is significantly smaller than the coefficient of variation of 0.54 reported by Park [1].

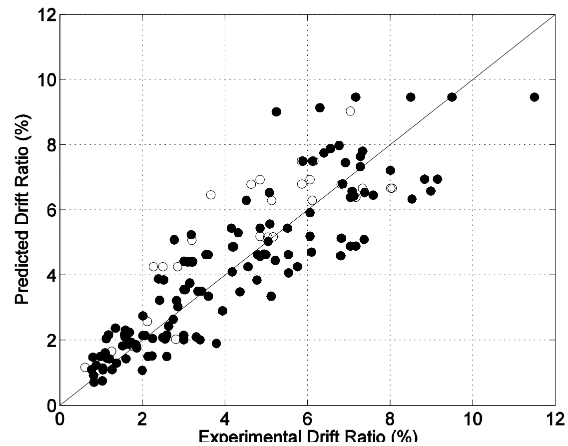

Figure 9. Comparison between experimental and predicted drift ratios

Figure 9 compares the drift ratios at failure obtained from experimental results with the estimated drift ratio capacities, $D\hat{R}_c$. The 45 degree line represents *DI*=1. As shown, there is a good agreement between the experimental and the predicted values. The censored data represent experimental results in which failure was not observed and, as expected, the predicted drift ratio capacities for most of these specimens are above the 45 degree line.

Effect of longitudinal reinforcement

Inclusion of ρ_t in the model did not reduce the scatter in estimating *DI*. This could be attributed in part to the fact that the specimens used in this study have equal reinforcement in tension and compression, and as a result a change in ρ_t may not have considerably affected their deformability. Of course, the amount of longitudinal reinforcement in a specimen affects the shear force demand on the specimen that can in turn affect the mode of failure of the specimen.

Effect of displacement history

The history of applied deformation can have significant effect on the deformation capacity of specimens (Pujol [16]). One may make use of the dissipated energy as a measure to account for such effect. Figure 10 shows the effect of the dissipated energy on the drift capacity of specimens. Each dot in the figure represents the ratios of the dissipated energies and drift ratio capacities for two identical specimens under different displacement histories. As it can be seen, a larger amount of dissipated energy is not necessarily associated with a smaller deformation capacity. This, by no means, should be interpreted as the lack of correlation between the history of loading and the deformation capacity. Figure 10, may merely

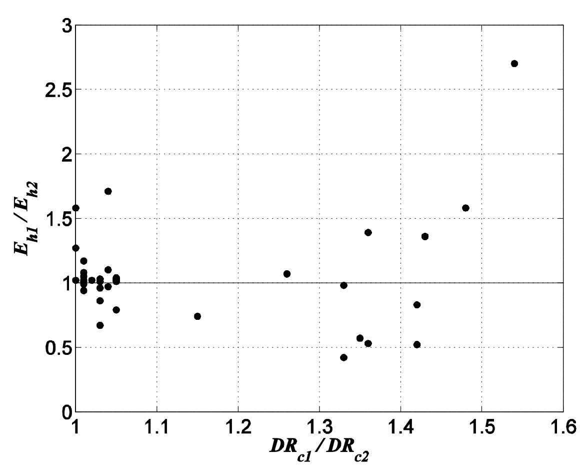

Figure 10. Dissipated energy vs. drift capacity

suggest that the dissipated energy may not be a reliable measure for accounting for the effects of displacement history on the deformation capacity of RC specimens.

Figure 11 shows the force-drift ratio relationships for three identical specimens (Murakami [3]). In specimen No. 86 one cycle is applied at each level of deformation. In specimen No. 88, however, four cycles are applied in the first two levels of deformations. As it can be seen, the behavior of the two specimens after these cycles is almost the same. The DR_c for both specimens are equal to 5.1%, while the dissipated energy in Specimen No. 88 is about 58% more than that in specimen No. 86. In specimen No. 87, the repeated cycles are applied at a larger drift, compared to that of specimen No. 88. As a result, the drift ratio capacity of this specimen is reduced to 3.6%. These test results suggest that perhaps there is a drift beyond which, repeated cycles results in a considerable drop in the strength capacity of RC specimens (Wight [44]).

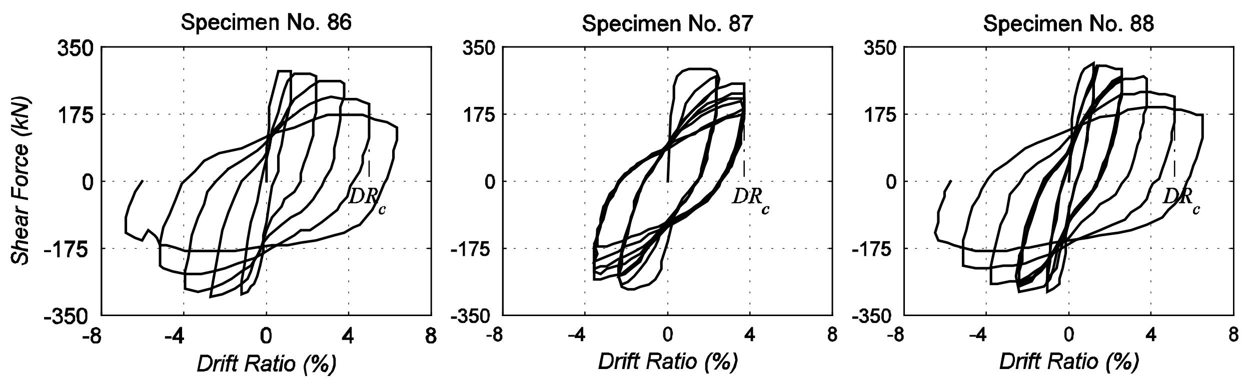

Figure 11. Effect of loading history on drift capacity

There is however, a need to account for the effects of displacement history on *DI*. In this paper a damage index is developed for specimens under cyclic displacements. A specimen is considered as been subjected to cyclic displacements if the specimen has experienced positive and negative drifts at least equal to 1/2 of the drift capacity of the specimen, prior two the half cycle that leads to the failure of the specimen. Note that all the specimens used in this paper have experienced cyclic displacements, as defined here.

CONCLUSIONS

In this paper, a new damage index for RC elements under cyclic loading is proposed. The model is based on estimating drift ratio capacity under cyclic displacements and does not utilize monotonic response of elements, since the mode of failure under monotonic and cyclic displacements may be different. The correlation coefficient in estimating the damage index is about 0.30 which is considerably smaller than 0.54 reported by Park [1]. In the model, the effect of the concentration of damage on one end of double curvature or double ended specimen is accounted for.

Although the displacement history can have significant effect on the response of RC elements, examining the effect of energy dissipation on the drift capacity of elements, it is concluded that the dissipated energy may not be a reliable measure for accounting for such effect.

REFERENCES

1. Park YJ, Ang AHS. "Mechanistic seismic damage model for reinforced concrete." Journal of Structural Engineering, ASCE, 1985; 111(4): 722-739.
2. Watanabe H, Kawano H. "Shear strength of RC members under load reversals." Proceedings of the 3rd International Conference on Fracture Mechanics of Concrete Structures (FRAMCOS-3), Gifu, Japan, 1998: 717-726.
3. Murakami M, Imai H. "A study on influence of different loading histories on failure behavior of R/C columns yielding in flexure." Transactions of the Japan Concrete Institute, 1986; 8: 367-380.
4. Morimoto H, Kuribayashi H, Fujii S, Morita S. "Local bond-slip behavior under splitting bond-shear failure of RC columns." Transactions of the Japan Concrete Institute, 1984; 6: 469-476.
5. Mugurama H, Tominaga M, Watanabe F. "Analytical and experimental studies on the deformation evaluation of reinforced concrete columns under seismic forces." International Association for Bridge and Structural Engineering (IABSE) Symposium: Resistance and ultimate deformability of structures acted on by well defined repeated loads, Lisboa, Portugal, 1973; 67-72.
6. Hirosawa M. "A list of past experimental results of reinforced concrete columns." Building Research Institute, Ministry of Construction of Japan, 1973.
7. Brown RH. "Reinforced concrete cantilever beams under slow cyclic loadings." PhD thesis, Rice University, Houston, Texas, 1970.
8. Ikeda A. "Load-deflection characteristics of reinforced concrete columns subjected to alternate loading." Report of the Training Institute for Engineering Teachers, Yokohama National University, Kanagawa, Japan, 1968.
9. Burns NH. "Load deformation characteristics of beam-column connections in reinforced concrete." PhD thesis, University of Illinois at Urbana-Champaign, Illinois, 1962.
10. Park YJ, Ang AHS, Wen YK. "Damage limiting aseismic design of buildings." Earthquake Spectra, 1987; 3(1): 1-26.
11. Cosenza E, Manfredi G, Ramasco R. "The use of damage functionals in earthquake engineering: a comparison between different procedures." Earthquake Engineering and Structural Dynamics, 1993; 22: 855-868.
12. Sasani M, Bazan M. "Damage model for reinforced concrete elements." Proceedings of the 9th International Conference on Applications of Statistics and Probability in Civil Engineering (ICASP9), San Francisco, California 2003; 1: 637-644.
13. Paulay T, Priestley MJN. "Seismic design of reinforced concrete and masonry buildings." John Wiley & Sons, New York, 1992.
14. Park R, Paulay T. "Reinforced Concrete Structures." Wiley-Interscience, John Wiley & Sons, New York, 1975.
15. Eberhard M. "Structural Performance Database." <http://maximus.ce.washington.edu/~peera1/>. University of Washington, 2004.
16. Pujol S. "Drift capacity of reinforced concrete columns subjected to displacement reversals." PhD thesis, School of Civil Engineering, Purdue University, Indiana, 2002.
17. Sezen H, Moehle JP. "Seismic behavior of shear-critical reinforced concrete building columns." Proceedings of the 7th U.S. National Conference on Earthquake Engineering, Boston, Massachusetts, 2002. CD-Rom. Earthquake Engineering Research Institute.
18. Mo YL, Wang SJ. "Seismic behavior of RC columns with various tie configurations." Journal of Structural Engineering, ASCE, 2000; 126(10): 1122-1130.
19. Aboutaha RS, Engelhardt MD, Jirsa JO, Kreger ME. "Rehabilitation of shear critical concrete columns by use of rectangular steel jackets." ACI Structural Journal, 1999; 96(1): 68-78.
20. Matamoros A. "Study of drift limits for high-strength concrete columns." PhD thesis, Department of Civil Engineering, University of Illinois at Urbana-Champaign, Illinois, 1999.
21. Saatcioglu M, Grira M. "Confinement of reinforced concrete columns with welded reinforcement grids." ACI Structural Journal, 1999; 96(1): 29-39.
22. Wehbe S, Saiidi MS, Sanders D. "Confinement of rectangular bridge columns for moderate seismic areas." Multidisciplinary Center for Earthquake Engineering Research Bulletin, 1998; 12(1).
23. Lynn A, Moehle JP, Mahin SA, Holmes WT. "Seismic evaluation of existing reinforced concrete buildings columns." Earthquake Spectra, 1996; 12(4): 715-739.

24. Nosho K, Stanton J, MacRae G. "Retrofit of rectangular reinforced concrete columns using Tonen Forca Tow Sheet carbon fiber wrapping." Report No. SGEM 96-2, Department of Civil Engineering, University of Washington, Seattle, 1996.
25. Park R, Paulay T. "Use of interlocking spirals for transverse reinforcement in bridge columns." Strength and ductility of concrete substructures and bridges, Road Research Unit Bulletin, 1990; 1(84): 77-92.
26. Tanaka H, Park R. "Effect of lateral confinement reinforcement on the ductile behavior of reinforced concrete columns." Report 90-2, Department of Civil Engineering, University of Canterbury, New Zealand, 1990.
27. Arakawa T, Arai Y, Mizoguchi M, Yoshida, M. "Shear resisting behavior of short reinforced concrete columns under biaxial bending-shear." Transactions of the Japan Concrete Institute, 1989; 11: 317-324.
28. Ono A, Shirai N, Adachi H, Sakamaki Y. "Elasto-plastic behavior of reinforced concrete columns with fluctuating axial force." Transactions of the Japan Concrete Institute, 1989; 11: 239-246.
29. Saatcioglu M, Ozcebe G. "Response of reinforced concrete columns to simulated seismic loading." ACI Structural Journal, 1989; 86(1):3-12.
30. Watson S, Park R. "Design of reinforced concrete frames of limited ductility." Report 89-4, Department of Civil Engineering, University of Canterbury, New Zealand, 1989.
31. Azizinamini A, Johal LS, Hanson NW, Musser DW, Corley WG. "Effects of transverse reinforcement on seismic performance of columns – a partial parametric investigation." Project No. CR-9617, Construction Technology Laboratories, Skokie, Illinois, 1988.
32. Kanda M, Shirai N, Adachi H, Sato T. "Analytical study on elasto-plastic hysteretic behaviors of reinforced concrete members." Transactions of the Japan Concrete Institute, 1988; 10: 257-264.
33. Imai H, Yamamoto Y. "A study on causes of earthquake damage of Izumi high school due to Miyagi-Ken-Oki Earthquake in 1978." Transactions of the Japan Concrete Institute, 1986; 8: 405-418.
34. Soesianawati MT, Park R, Priestley MJN. "Limited ductility design of reinforced concrete columns." Report 86-10, Department of Civil Engineering, University of Canterbury, New Zealand, 1986.
35. Zahn FA, Park R, Priestley MJN. "Design of reinforced bridge columns for strength and ductility." Report 86-7, Department of Civil Engineering, University of Canterbury, New Zealand, 1986.
36. Bett BJ, Klingner RE, Jirsa JO. "Behavior of strengthened and repaired reinforced concrete columns under cyclic deformations." PMFSEL Report No. 85-3, Department of Civil Engineering, University of Texas at Austin, Austin, Texas, 1985.
37. Ohue M, Morimoto H, Fujii S, Morita S. "The behavior of RC short columns failing in splitting bond-shear under dynamic lateral loading." Transactions of the Japan Concrete Institute, 1985; 7: 293-300.
38. Ohno T, Nishioka T. "An experimental study on energy absorption capacity of columns in reinforced concrete structures." Proceedings of the JCSE, Structural Engineering/Earthquake Engineering, 1984; 1(2):137-147.
39. Nagasaka T. "Effectiveness of steel fiber as web reinforcement in reinforced concrete columns." Transactions of the Japan Concrete Institute, 1982; 4: 493-500.
40. Umehara H, Jirsa JO. "Shear strength deterioration of short reinforced concrete columns under cyclic deformations." PMFSEL Report No. 82-3, Department of Civil Engineering, University of Texas at Austin, Austin, Texas, 1982.
41. Ghee AB, Priestley MJN, Park R. "Ductility of reinforced bridge piers under seismic loading." Report 81-3, Department of Civil Engineering, University of Canterbury, New Zealand, 1981.
42. Gill WD, Park R, Priestley MJN. "Ductility of rectangular reinforced concrete columns with axial load." Report 79-1, Department of Civil Engineering, University of Canterbury, New Zealand, 1979.
43. Atalay MB, Penzien J. "The seismic behavior of critical regions of reinforced concrete components as influenced by moment, shear and axial force." Report No. EERC 75-19, Earthquake Engineering Research Center, University of California, Berkeley, California, 1975.
44. Wight JK, Sozen MA. "Shear strength decay in reinforced concrete columns subjected to large displacements reversals." Structural Research Series No. 403, Civil Engineering Studies, University of Illinois at Urbana-Champaign, Illinois, 1973.
45. Lynn A. "Seismic evaluation of existing reinforced concrete building columns." PhD thesis, University of California at Berkeley, California, 2001.
46. Sasani M, Bazan M. "New deformation capacity and damage models for RC elements." Submitted for review and possible publication to Journal of Structural Engineering, ASCE, 2004.